

THELMA Code Analysis of Bronze Route Nb₃Sn Strand Bending Effect on I_c

P. L. Ribani, D. P. Boso, M. Lefik, Y. Nunoya, L. Savoldi Richard, B. A. Schrefler, and R. Zanino

Abstract—The THELMA (Thermal-Hydraulic-Electro-Magnetic) code has been developed with the aim of simulating the main aspects of superconductors to be used in the coils of the International Thermonuclear Experimental Reactor (ITER). An application of the code is presented here, where THELMA is used to simulate a single strand by considering, as cable elements, groups of superconducting (SC) filaments and the corresponding portion of the resistive matrix. This approach is used to reproduce the voltage-current characteristic of a Nb₃Sn bronze route strand when subject to a bending mechanical load. Attention is focused particularly on the effect of the applied mechanical load on the critical current, which is considered a relevant item in the explanation of the degradation of the coil performance observed in several ITER Model and Insert Coil experiments. The longitudinal strain of the SC filaments is calculated by means of a composite beam model of the strand, taking into account the nonlinear, temperature-dependent material characteristics of the components. The whole load history is simulated, computing first the thermal strain due to cool-down, and then the mechanical strain due to the bending at 4.2 K.

Index Terms—Bending strain, electromagnetic analysis, superconducting cables, superconducting magnets.

I. INTRODUCTION

THE ITER Model Coil and Insert Coil experiments showed a significant degradation of the current-carrying capability of the Nb₃Sn based Cable-in-Conduit conductor (CICC), with respect to the expectations coming from experimental data on a single strand, subject to pure tensile/compressive load [1]–[5]. Such a degradation can be due to the bending of the strands due to the Lorentz force and contact distribution [6] and experimental investigations performed at JAERI (Japan Atomic Energy Research Institute) Naka and elsewhere seem to confirm it [7], [8]. The THELMA code [9] has been developed with the support of EFDA (European Fusion Development Agreement) with the goal of simulating the relevant aspects of the ITER SC magnets, which utilize CICC cables. The code is based on a coupled electromagnetic and thermal-hydraulic model of the cable

Manuscript received September 20, 2005. This work was supported in part by EFDA-MIUR.

P. L. Ribani is with Dipartimento di Ingegneria Elettrica, Università di Bologna, 40136 Bologna, Italy (e-mail: pierluigi.ribani@mail.ing.unibo.it).

D. P. Boso and B. A. Schrefler are with Dipartimento di Costruzioni e Trasporti, Università di Padova, 35131 Padova, Italy (e-mail: boso@dic.unipd.it; bas@dic.unipd.it).

M. Lefik is with the Technical University of Łódź, 93-590 Lodz, Poland (e-mail: emlefik@mail.p.lodz.pl).

Y. Nunoya is with JAERI, Naka, Japan (e-mail: nunoya@naka.jaeri.go.jp).

L. Savoldi Richard and R. Zanino are with Dipartimento di Energetica, Politecnico, I-10129 Torino, Italy (e-mail: laura.savoldi@polito.it; roberto.zanino@polito.it).

Digital Object Identifier 10.1109/TASC.2006.873337

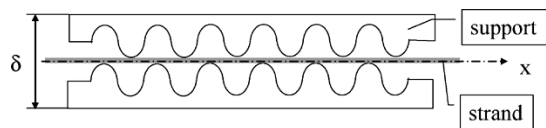


Fig. 1. Experimental layout.

and joints. The electromagnetic (EM) model of the cable is of the distributed parameters circuit type and calculates the current distribution with reference to the cable-elements (CE) of the model which represent a strand or a group of strands of the cable. The code can be utilized to model the Voltage-Current (V-I) curve of a Nb₃Sn strand subject to the bending load as reported in [7]. In this case a CE represents a group of SC filaments in the strand and their corresponding matrix material. To calculate the critical current density of the SC material, the strain inside each CE is needed. The computation of the SC filaments strain is done using an asymptotic homogenization technique as described in [10], [11] and modeling the strand as a *beam*. Three different kinematical hypotheses are taken into consideration: Kirchhoff model, Timoshenko theory and the composite fibrous beam formulation described in [12].

A. Experimental Setup

The set-up of the experiments performed at JAERI is fully described in [7] and shown schematically in Fig. 1.

A Nb₃Sn strand sample, 110 mm long, was tested under bending mechanical load. Different loads were obtained by changing the distance (δ) between the upper and lower part of the stainless steel support and the critical current of the sample was measured based on the critical electric field $E_c = 10 \mu\text{V}/\text{m}$. The sample was in a liquid helium bath at 4.2 K and it was subject to an external 11 T magnetic flux density in the z-direction. The strand was a bronze-route one fabricated by Furukawa Co; its cross section is shown in Fig. 2 [13]. The same strand was used in the CS Insert Coil. The strand diameter is 0.81 mm and 313 groups of 19 Nb₃Sn filaments each are embedded in a bronze core with a diameter of 0.501 mm. The core is separated from the external Cu stabilizer by a tantalum barrier. The ratio χ between the matrix material (bronze) and the SC material in the core is about 2.0. The twist pitch of the SC filaments is 20 mm.

II. MODEL

The strand model presented here couples an electromagnetic description, based on the THELMA code, with a detailed finite element mechanical analysis, as discussed below.

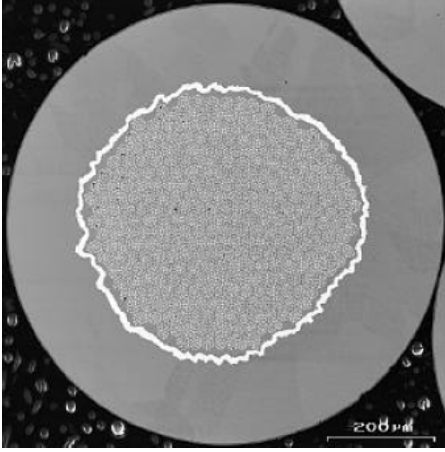


Fig. 2. Cross section of the Furukawa strand.

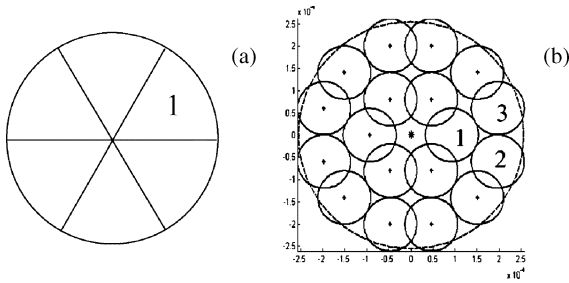


Fig. 3. Cross section of the strand core in the 6 CE model (a) and in the 18 CE model (b).

A. THELMA Code Model

Only the bronze + SC core is considered since the current flowing through the copper annulus is negligible in the experimental range. Two geometrical models of the strand core are utilized. The first model considers 6 CE which completely cover the cross section of the strand core without overlapping, as shown in Fig. 3(a). The second model, shown in Fig. 3(b), considers 18 CE with circular cross section which have the same matrix/SC ratio as the strand core; in this case the CE partially overlap each other [14]. The twist pitch of all the cable-elements is 20 mm.

The transverse conductivity per unit length between CE is calculated from the assumed value of the matrix electrical resistivity $\rho_m = 10^{-8} \Omega\text{m}$. The end regions of the strand are connected to the power supply. A simple resistive termination model is used in this case while the central part of the strand, 80 mm long, is modeled by means of the distributed parameters circuit cable model of the THELMA code [15]. To obtain convergence, a uniform mesh of 65 nodes ($\Delta x = 1.25 \text{ mm}$) has been utilized; doubling the nodes showed a negligible change in the calculated critical current of the strand. The temperature is 4.2 K, constant in time and uniform in space. This hypothesis is justified in view of the large thermal coupling between the strand and the heat capacity of the helium bath; the temperature increase due to the joule energy deposition corresponding to the strand carrying 160 A at the critical electric field for 10 s is estimated $\sim 0.1 \text{ K}$, which is negligible here.

The SC E – J characteristics is supposed to be of the power law type

$$E = E_c \left(\frac{J_s}{J_c} \right)^n \quad (1)$$

with $E_c = 10 \mu\text{V}/\text{m}$. In (1) J_s is the current density in the SC; which is related to the value J of the so-called engineering current density (current divided by total strand area), by

$$E = E_c \left(\frac{J_s}{J_c} \right)^n = \rho_m J_m; \quad J_s \frac{1}{1+\chi} + J_m \frac{\chi}{1+\chi} = J \quad (2)$$

where J_m is the current density in the matrix material. The critical current density J_c is a function of the magnetic flux density B , temperature T and strain ε .

$$J_c = \frac{C_0}{\sqrt{B}} F(B, T, \varepsilon) \quad (3)$$

Generally the strain to be considered in the critical current density calculation should take into account the tensorial nature of the strain. In this case only the longitudinal strain is considered, since, from the mechanical calculations, it results that this component is much higher than the others. Many correlations can be found in literature for the critical current density scaling law [16]–[20] and discussion is not completely closed. In this work, as a first attempt, the simple and well defined Summers scaling [16] is utilized with critical parameters $T_{c0m} = 18.3 \text{ K}$ and $B_{c20m} = 28.7 \text{ T}$. As to C_0 , it is usually considered as a fitting parameter; many authors define indeed by means of (3) the non-Cu critical current density and the value of C_0 must be derived from experimental characterization of the particular strand. In this work a slightly different approach is used; consistent with (1), C_0 is considered a property of SC filaments only, thus (3) defines the critical current density in the SC. The content of Sn in the SC, in the bronze-route Nb_3Sn strands, is not constant and depends on the forming process [17]. Thus a characterization of the strand is always necessary. The value of $C_0 = 3.05 \times 10^{10} \text{ AT}^{0.5}/\text{m}^2$ is then obtained by fitting the calculated I_c with the 6 CE model to the experimental one, measured when no bending load is applied. Unfortunately, the utilized scaling law (3) is accurate only for a limited range of values of the strain. Fig. 4 shows the normalized current density (which is equal to 1 when $\varepsilon = 0$) calculated by the adopted Summers scaling (3) compared with the Hampshire scaling law, as reported in [20]. For strain approaching 1% and larger, the two scaling laws differ significantly. In the present work, for strain values larger than $\pm 1\%$ the SC material is assumed to be a normal material with a constant resistivity given by $60 \times 10^{-8} \Omega\text{m}$ [17]. Consistent with the model, the strain ε considered in (3), is also the longitudinal strain of the SC filaments only, and is different from the strain of the bronze matrix or of the copper annulus.

Even if data for the dependence of the n -value on B , T and ε , can be found in the literature [14], [15], they are mostly given in graphic form and it is difficult to obtain an algebraic relation. Moreover it has been shown in [7] that one of the main mechanisms for the reduction of the n -value in the JAERI experiments is the current redistribution among the SC filaments. Thus, in this work, a constant value equal to the experimental

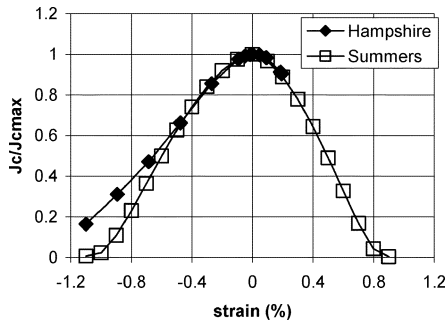


Fig. 4. Summers scaling law compared with Hampshire one.

TABLE I
MINIMUM AND MAXIMUM VALUES OF THE SC STRAIN IN THE CROSS SECTION OF THE STRAND VS. DISPLACEMENT

$\Delta\delta$ (mm)	Minimum strain (%)	Maximum strain (%)
0.000	-0.247	-0.247
0.025	-0.612	0.358
0.050	-1.029	1.020
0.075	-1.457	1.699
0.100	-1.891	2.387
0.150	-2.728	3.716
0.200	-3.566	5.047

one ($n = 28.2$) when no bending load is applied ($\Delta\delta = 0$) is utilized.

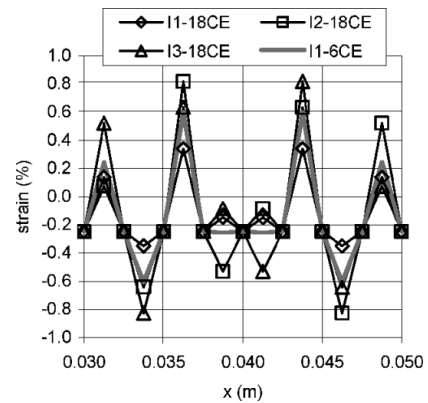
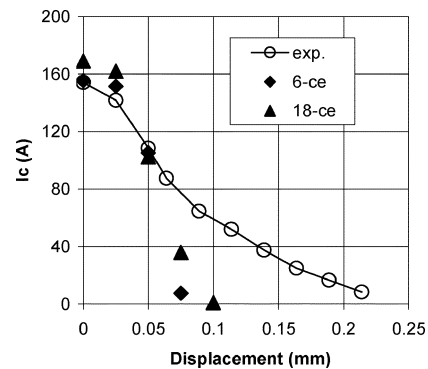
B. Mechanical Model

The strand behavior is modeled as that of a *beam* and it is further assumed that its cross section remains circular. Beam theories are based on the main hypothesis that transversal sections remain plane all over the deformation process. The cross section of the strand is made of only two materials: the outer ring of copper and the inner area, endowed with the characteristics resulting from the homogenization. The solution is obtained first prescribing the beam-type kinematical hypothesis and then integrating over the given cross section the generalized forces (bending moments, axial and shear forces). The study is presented in detail in a companion paper [21].

III. SIMULATION RESULTS AND DISCUSSION

The critical current (I_c) and the n -value corresponding to different values of $\Delta\delta$, in the range 0–0.2 mm, have been calculated assuming a strand current rump-up of 1 A/s. The integral of the electric field along each CE axis from $x = 7.5$ mm (first voltage tap position) to $x = 72.5$ mm (second voltage tap position) is calculated with the THELMA code. The average overall calculated values (as many as the CE) is then compared with the measured voltage. The critical voltage is $0.65 \mu\text{V}$. The n -value is calculated by considering the V-I curve in the range $V = 0.65 \mu\text{V} - 6.5 \mu\text{V}$.

Table I reports the minimum and maximum values of the longitudinal strain in the strand calculated with different $\Delta\delta$ according to Kirchhoff and Timoshenko beam model (Kirchhoff and Timoshenko approaches give the bounds inside which

Fig. 5. Strain distribution of CE n.1 [Fig. 3(a)] and CE n. 1-3 [Fig. 3(b)] when $\Delta\delta = 0.05$ mm.Fig. 6. Calculated and experimental value of the critical current vs. $\Delta\delta$.

each beam model should fall and the third model gives results very close to those obtained using Kirchhoff hypothesis [21]). Since the cross section remains plane, the strain is a linear function of z -coordinate only, and its maximum and minimum value can be found in the upper ($z = 0.255$ mm) or lower edge ($z = -0.255$ mm). Fig. 5 shows the calculated strain for CE n. 1 in the 6 CE model and CE n. 1-3 in the 18 CE model, when $\Delta\delta = 0.05$ mm; it can be seen that this case corresponds to the limit case where the Summers scaling law is supposed to be reliable in the modeling of the experimental data. For $\Delta\delta \geq 0.1$ mm the calculated strain values exceed also the validity range of the Hampshire scaling law.

The calculated values of the critical current and of the n -value with different $\Delta\delta$ are shown in Figs. 6 and 7. In the range of applicability of the scaling law (3), with reference to the critical current values, the agreement with the experimental data is good with both models (relative error $\leq 15\%$). It is large (50% for the 18 CE model, 90% for the 6 CE model) for $\Delta\delta = 0.075$ mm. For $\Delta\delta \geq 0.1$ mm both models were unable to reproduce the experimental results. One of the reasons is surely the inadequacy of the scaling law (3); nevertheless the calculated strain is so large that the Hampshire scaling law would not be adequate either. Other reasons could be responsible for the discrepancy: the breaking of the filaments is not taken into account in the mechanical calculations and also the hypothesis of circular cross section of the strands can be no more valid (in this regime, $\Delta\delta$

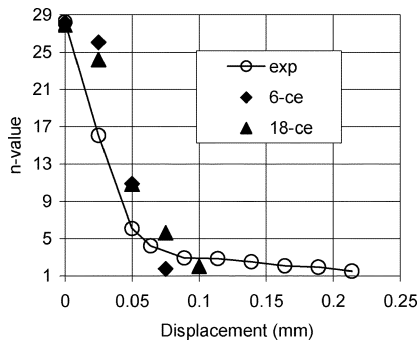


Fig. 7. Calculated and experimental n-value vs. $\Delta\delta$.

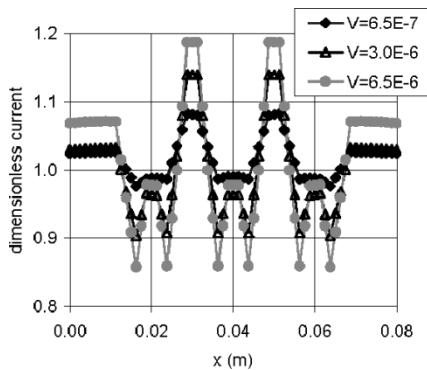


Fig. 8. Calculated dimensionless current for CE n. 1 [Fig. 3(a)] when $\Delta\delta = 0.05$ mm, in correspondence to different values of the voltage.

is more than 20% of the strand diameter). More investigation is required.

With reference to the n-value and limiting the considerations to the range $\Delta\delta < 0.05$ mm, the error between the calculated and experimental data is large. Nevertheless the calculations show a reduction of the n-value of the strand qualitatively similar to the experiment, even considering the n-value of the SC filaments independent from the strain. The reduction of n at increasing load is due to the redistribution of the current among the CE. As an example, the change in the distribution of the dimensionless current of a CE during the simulation corresponding to $\Delta\delta = 0.05$ mm with the 6 CE model is shown in Fig. 8. The dimensionless current is defined for any CE as the ratio between the computed current and the current which would be carried by that CE if the current would be uniformly distributed over the strand cross-section. A significant redistribution of the current can be observed in the figure which is not present when $\Delta\delta = 0$. In order to completely reproduce the experimental data of the n-value, its dependence on the strain should then be considered.

IV. CONCLUSION

The THELMA code was used to simulate I_c experiments on a Nb_3Sn strand under bending mechanical load. The critical cur-

rent density of the SC was calculated by means of the Summers scaling law considering the longitudinal strain of the SC filaments. The strain values were obtained considering the strand as a beam and using the asymptotic homogenization theory. Computed I_c agree with the experimental ones within a relative error of 15%, for values of the displacement corresponding to strain in SC filaments below the 1% range. Only qualitative agreement has been obtained for the n-value in the same range of strain.

REFERENCES

- [1] R. Zanino *et al.*, "Performance evaluation of the ITER toroidal field model coil phase I. Part 1: Current sharing temperature measurement," *Cryogenics*, vol. 43, pp. 79–90, 2003.
- [2] R. Zanino and L. Savoldi Richard, "Performance evaluation of the ITER toroidal field model coil phase I. Part 2: M&M analysis and interpretation," *Cryogenics*, vol. 43, pp. 91–100, 2003.
- [3] R. Zanino *et al.*, "Tcs tests and performance assessment of the ITER toroidal field model coil (phase II)," *IEEE Trans. Appl. Supercond.*, vol. 14, pp. 1519–1522, 2004.
- [4] —, "Analysis and interpretation of the full set (2000-2002) of tcs tests in Conductor 1A of the ITER central solenoid model coil," *Cryogenics*, vol. 43, pp. 179–197, 2003.
- [5] N. Martovetsky *et al.*, "Test of the ITER central solenoid model coil and CS insert," *IEEE Trans. Appl. Supercond.*, vol. 12, pp. 600–605, 2002.
- [6] N. Mitchell, "Mechanical and magnetic load effects in Nb_3Sn cable-in-conduit conductors," *Cryogenics*, vol. 43, pp. 255–270, 2003.
- [7] Y. Nunoya, "Experimental investigation on the effect of transverse electromagnetic force on the v-t curve of the CIC conductor," *IEEE Trans. Appl. Supercond.*, vol. 14, pp. 1468–1472, 2004.
- [8] A. Nijhuis *et al.*, "Effect of periodic cyclic deformation on the voltage current transition of Nb_3Sn strands tested in the novel 'TARSIS' setup," *IEEE Trans. Appl. Supercond.*, vol. 14, pp. 1464–1467, 2004.
- [9] F. Bellina *et al.*, "Superconducting cables current distribution analysis," *Fus. Eng. Des.*, vol. 66–68, pp. 1159–1163, 2003.
- [10] D. P. Boso *et al.*, "A multilevel homogenized model for superconducting strand thewrmomechanics," *Cryogenics*, vol. 45, pp. 259–271, 2005.
- [11] —, "Homogenization methods for the thermo-mechanical analysis of Nb_3Sn based strand," *Cryogenics*, to be published.
- [12] M. Lefik and B. A. Schrefler, "3D finite element analysis of composite beams with parallel fibers based on the homogenization theory," *Computational Mechanics*, vol. 14, no. 1, pp. 2–15, 1994.
- [13] P. Lee, 3rd ITER Benchmark—UW-ASC Cu:Non-Cu..
- [14] M. Breschi *et al.*, "Analysis of inductance coefficients in multistrand cables: analytical, numerical and experimental results," *IEEE Trans. Appl. Supercond.*, vol. 15, pp. 3797–3807, 2005.
- [15] P. L. Ribani, "CDCABLE: a code to calculate current distribution in superconducting multi-filamentary cables," TASK N. TW0-T400-1/101 Deliverable N.8 Univ. of Bologna, 2002.
- [16] L. T. Summers *et al.*, "A model for the prediction of Nb_3Sn critical current as a function of field, temperature, strain, and radiation damage," *IEEE Trans. Magn.*, vol. 27, pp. 2041–2044, 1991.
- [17] A. Godeke, "Performance Boundaries in Nb_3Sn Superconductors," Ph.D. thesis, Univ. of Twente, , 2005, ISBN 90-365-2224-2.
- [18] A. Godeke *et al.*, "Toward an accurate scaling relation for critical current in niobium-tin conductores," *IEEE Trans. Appl. Supercond.*, vol. 12, pp. 1029–1032, 2002.
- [19] N. Cheggour and D. P. Hampshire, "The unified strain and temperature scaling law for the pinning force density of bronze-route Nb_3Sn wires in high magnetic fields," *Cryogenics*, vol. 42, pp. 299–309, 2002.
- [20] D. M. Taylor and D. P. Hampshire, "Numerical values for J_c of a VAC wire as function of strain at 4.2 K in high magnetic fields," [Online]. Available: <http://www.dur.ac.uk/superconductivity.durham>.
- [21] D. P. Boso *et al.*, "Thermal and bending strain on Nb_3Sn based strands," *IEEE Trans. Appl. Supercond.*, to be published.